J. Cell. Mol. Med. Vol 13, No 9B, 2009 pp. 3358-3369

Presenilin-2 dampens intracellular Ca^{2+} stores by increasing Ca^{2+} leakage and reducing Ca^{2+} uptake

Lucia Brunello †, Enrico Zampese †, Cristina Florean, Tullio Pozzan, Paola Pizzo*, Cristina Fasolato*

Department of Biomedical Sciences, University of Padova, Padova, Italy

Received: December 23, 2008; Accepted: March 10, 2009

Abstract

We have previously shown that familial Alzheimer's disease mutants of presenilin-2 (PS2) and, to a lesser extent, of presenilin-1 (PS1) lower the Ca^{2+} concentration of intracellular stores. We here examined the mechanism by which wild-type and mutant PS2 affect store Ca^{2+} handling. By using HeLa, SH-SY5Y and MEFs as model cells, and recombinant aequorins as Ca^{2+} probes, we show evidence that transient expression of either wild-type or mutant PS2 increases the passive Ca^{2+} leakage: both ryanodine- and IP_3-receptors contribute to Ca^{2+} exit out of the ER, whereas the ribosome translocon complex is not involved. In SH-SY5Y cells and MEFs, wild-type and mutant PS2 potently reduce the uptake of Ca^{2+} inside the stores, an effect that can be counteracted by over-expression of SERCA-2B. On this line, in wild-type MEFs, lowering the endogenous level of PS2 by RNA interference, increases the Ca^{2+}-loading capability of intracellular stores. Furthermore, we show that in PS double knockout MEFs, reduction of Ca^{2+} stores is mimicked by the expression of PS2-D366A, a loss-of-function mutant, uncleaved because also devoid of presenilinase activity but not by co-expression of the two catalytic active fragments of PS2. In summary, both physiological and increased levels of wild-type and mutant PS2 reduce the Ca^{2+} uptake by intracellular stores. To exert this newly described function, PS2 needs to be in its full-length form, even if it can subsequently be cleaved.

Keywords: presenilin • calcium stores • Alzheimer's disease • SERCA • aequorin

Introduction

Alzheimer's disease (AD) is responsible for the most part of the dementias in developed countries. Although the majority of AD cases are sporadic, a significant fraction of AD is inherited in a dominant pattern. The familial forms of AD (FAD) have been traced to mutations in genes for three proteins: the amyloid precursor protein (APP), presenilin-1 and -2 (PS1 and 2). PSs are essential components of the γ-secretase complex which, in turn, by cleaving APP in concert with β-secretase, produces the neurotoxic β-amyloid peptide (Aβ).

Much attention has recently been devoted to the fact that some FAD-linked PS mutants cause a dysregulation of cellular Ca^{2+} homeostasis. Ca^{2+} is a key parameter in neuronal physiopathology, as it controls many cellular functions, whereas alterations in Ca^{2+} levels are responsible for neuronal cell death in a number of genetic and sporadic diseases. It has been suggested that an imbalance of Ca^{2+} homeostasis may represent an early event in the pathogenesis of FAD, but the mechanisms through which FAD-linked PS mutants affect the control of cellular Ca^{2+} are controversial. In particular, it was observed that mutations in PS1 cause larger Ca^{2+} release from intracellular stores and increase excitotoxicity in neurons from transgenic mice [1–5]. The idea that FAD-linked PS mutations are somehow correlated to altered Ca^{2+} signalling was further supported by the fact that these mutations could alter the expression, or sensitivity, of endoplasmic reticulum (ER) Ca^{2+} release channels, ryanodine receptors (RyRs) and inositol (1,4,5)-trisphosphate receptors (IP_3Rs) in different cell models [2, 6–11] and in neurons from AD mice [5, 12, 13]. Interestingly, similar observations were also made in non-neuronal cells, such as fibroblasts, lymphocytes and oocytes, indicating that PSs play a

†These authors contributed equally to this work.
*Correspondence to: Cristina FASOLATO,
Department of Biomedical Sciences,
Via G. Colombo 3, 35121 Padova, Italy.
Tel.: +39-049-827.6065
Fax: +39-049-827.6049
E-mail: cristina.fasolato@unipd.it

Paola PIZZO,
Department of Biomedical Sciences,
Via G. Colombo 3, 35121 Padova, Italy
Tel: +39-049-827.6065
Fax: +39-049-827.6049
E-mail: paola.pizzo@unipd.it

doi:10.1111/j.1582-4934.2009.00755.x

general role in Ca^{2+} homeostasis [11, 14]. These data lead to the 'Ca^{2+} overload' hypothesis [15, 16], stating that AD neuronal degeneration depends on exaggerated ER Ca^{2+} release because of ER Ca^{2+} overload. However, an increased ER Ca^{2+} content has not always been observed: different studies have described either no alteration or reduced ER Ca^{2+} stores in cells expressing wild-type (wt) or FAD-mutant PSs [11, 17–19]. In particular, we demonstrated that the FAD-linked PS2 mutations M239I and T122R reduce rather than increase Ca^{2+} release in fibroblasts from FAD patients and in cell lines stably or transiently expressing the PS2 mutants [18, 20, 21]. In addition, an extended investigation of other FAD-linked PS mutants (PS2−N141I, PS1-A246E, PS1-L286V, PS1-M146L, PS1-P117L), by monitoring directly the ER Ca^{2+} levels in different cell lines, confirmed that these FAD-linked PS2 mutations caused a reduction in ER Ca^{2+} levels and none of the PS1 mutations caused an increase [18].

Recently, a physiological role for wt PSs in ER Ca^{2+} handling has also been proposed, although divergent and contrasting data were reported [11, 18, 22–25]. In agreement, different mechanisms of PSs action have been proposed to explain their effect on Ca^{2+} homeostasis. PSs were demonstrated to form Ca^{2+} permeable channels in planar lipid bilayers [23], with FAD-linked PS mutants forming channels with reduced ionic conductance and thus being responsible for ER Ca^{2+} overload [23, 26]. An increased Ca^{2+} content has been also explained by an increased sarco-endoplasmic reticulum calcium-ATPase (SERCA)-2B activity, as deduced by accelerated cytosolic Ca^{2+} clearance following expression of wt PS1/2 or PS1−M146V in *Xenopus laevis* oocytes [25]. In contrast, Cheung *et al.* demonstrated that different FAD PS mutants increase IP_3Rs' sensitivity, leading to exaggerated Ca^{2+} responses, yet in the presence of reduced ER Ca^{2+} levels [11].

By employing different cell models, we here show that wt and mutant PS2 act primarily by reducing SERCA pumps' activity and secondly by increasing the leak across ER Ca^{2+} channels (RyRs and IP_3Rs).

Materials and methods

Cell lines and transfection

HeLa and SH-SY5Y cells were grown in DMEM supplemented with 10% FCS containing penicillin (100 U/ml) and streptomycin (100 μg/ml). Before transfection, cells were seeded on cover slips (13-mm-diameter) and allowed to grow to 50% confluence. At this stage, transfections of HeLa cells were carried out using the Ca^{2+}-phosphate technique in the presence of 4 μg of DNA (3 μg PS2-cDNA or void vector plus 1 μg aequorin [Aeq] cDNA). SH−SY5Y cells were transfected by means of Lipofectamine™ 2000 using 1.5 μg of DNA (1 μg PS2-cDNA or void vector plus 0.5 μg Aeq cDNA). Intracellular Ca^{2+} measurements were carried out 48 or 24 hrs after transfection by means of the Aeq technique as previously described [27] and summarized below. PS1/PS2-null ($PS1^{-/-}$, $PS2^{-/-}$) and wild-type mouse embryonic fibroblasts (MEFs), obtained as previously described [28, 29], were kindly provided by Dr. Bart De Strooper (Center for Human Genetics, KUL, VIB, Leuven, Belgium). Cells, grown in DMEM-F12 supplemented with 10% FCS and 100 U/ml penicillin/streptomycin, were transfected by Lipofectamine™2000 employing 2 μg of DNA (1.5 μg PS2-cDNA or void vector plus 0.5 μg Aeq cDNA). For γ-secretase activity assay [30] cells were transfected with 1.5 μg of PS2-cDNA and 0.5 μg of C99-GFP instead of Aeq. For RNA interference experiments, the growth medium was substituted 1 hr before transfection with antibiotics-free medium; siRNAs (murine IP_3R-1 [GenBank accession no. NM-010585; nucleotides 505–523, 2254–2272, 3680–3698 and 5122–5140] and IP_3R-3 [GenBank accession no. NM-080553; nucleotides 1114–1132, 1125–1143, 1219–1237 and 1459–1477]; mouse PS2, target sequence: GAUAUACUCAUCUGCCAUG; siGENOME RISC-Free Control siRNA; Dharmacon Research, Lafayette, CO) were added to the transfection mixes to a final concentration of 20–40 nM.

Ca^{2+} measurements

Cells seeded on 13-mm-diameter cover slips and transfected with Aeq constructs were incubated at 37°C with coelenterazine (5 μM) for 1–2 hrs in a modified Krebs–Ringer buffer (mKRB, in mM:140 NaCl, 2.8 KCl, 2 $MgCl_2$, 1 $CaCl_2$, 10 HEPES, 11 glucose, pH 7.4) and then transferred to the perfusion chamber. For reconstitution of ER-Aeq, luminal [Ca^{2+}] was reduced before coelenterazine addition by exposing the cells to CPA (20 μM) in mKRB without $CaCl_2$ (Ca^{2+}-free mKRB) and containing EGTA (600 μM). Upon 1-hr incubation at 4°C in the same medium, the cells were extensively washed with Ca^{2+}-free mKRB supplemented with EGTA (1 mM) and bovine serum albumin (BSA, 2%). All the luminescence measurements were carried out in mKRB at 37°C. For SH-SY5Y and MEF cells, a high potassium medium (in mM: KCl 100, NaCl 43, $MgCl_2$ 1, HEPES 10, pH 7.4) was used. The experiments were terminated by cell permeabilization with digitonin (100 μM) in a hypotonic Ca^{2+}-rich solution (10 mM $CaCl_2$ in H_2O) to discharge the remaining unused Aeq pool. The light signal was collected as previously described [27].

For permeabilization, cells were exposed for 1–2 min. to digitonin (20–100 μM) in an intracellular medium containing (in mM): KCl 130, NaCl 10, KH_2PO_4 1, succinic acid 2, $MgSO_4$ 1, HEPES 20, EGTA 0.05 pH 7, at 37°C. The cells were then washed with the same intracellular medium containing EGTA 50 μM for 2–5 min. The Ca^{2+}-buffer solution was prepared by adding to the intracellular medium: HEDTA, piruvic acid and $MgCl_2$ (1 mM each), EGTA or BAPTA (2 mM) and $CaCl_2$ at different concentrations (0.5−1.8 mM) and the pH was brought to 7 at 37°C. $ATPNa_2$ (0.2 mM) was added to this Ca^{2+}-buffered solution. The free [Ca^{2+}] (0.1–2 μM) was estimated by MaxChelator2.5 and checked by fluorimetric measurements with fura-2.

Plasmids

pcDNA3 vectors, codifying different PS2 mutants (M239I, N141I, T122R, D366A) were created by site-directed mutagenesis of pcDNA3/PS2-wt (QuikChange Site-directed mutagenesis Kit, Stratagene, La Jolla, CA). The constructs were checked by sequence analysis (ABI Prism Genetic Analyzer 310, Applied Biosystems, Monza, Italy).

Protein extracts preparation and Western blot analysis

The different cell types were harvested and treated as previously reported [21]. Briefly, cells were washed twice with ice-cold phosphate-buffered

saline (PBS) and harvested with RIPA buffer supplemented with proteases inhibitors cocktail (Complete Mini™, Roche, Basel, Schweiz). Samples were analysed in SDS−PAGE gel, and Western blotting immunodetection was carried out with the polyclonal antibody anti-PS2 (324–335; Ab-2, Calbiochem, Merck, Darmstadt, Germany) and with the monoclonal mouse antibody anti-PS2 (MMS-359S, Covance Research Products Inc., Princeton, NJ, USA). IP_3R-1 and -3 were detected by a polyclonal antibody (PA3–901A, ABR-Affinity BioReagents, Inc., Golden, CO, USA) and a monoclonal mouse antibody (610312, BD Biosciences Pharmingen, San Jose, CA, USA), respectively. SERCA-2B detection was carried out with a polyclonal anti-SERCA-2 antibody (N-19, Santa Cruz Biotechnology, Inc.). AICD-GFP was detected by the polyclonal anti-GFP antibody ab290, purchased from abCAM (Cambridge Science Park, Cambridge, UK). Actin was detected by the monoclonal mouse antibody (A4700, Sigma-Aldrich, St. Louis, MO, USA) The proteins were visualized by the chemiluminescence reagent ECL (Amersham, GE Healthcare, UK Ltd., Amersham Place, Little Chalfont, Buckinghamshire, UK).

Chemicals and reagents

Antibiotics, sera, culture media, plasmids and Lipofectamine™2000 were purchased from Invitrogen (Carlsbad, CA); DAPT and MW167 (γ-secretase inhibitor II) were from Calbiochem (Merck KGaA; Darmstadt, Germany), whereas all other reagents were from Sigma Chemical Co. (St. Louis, MO), unless otherwise stated.

Statistical analysis

Data were analysed by Origin 7.5 SR5 (OriginLab Corporation, Northampton/Wellesley Hills, MA, USA). Averages are expressed as mean ± S.E.M. (n = number of independent experiments; * = $P < 0.05$, ** = $P < 0.01$, *** = $P < 0.001$, unpaired Student's t-test).

Results

Effect of PS2 variants on store calcium leak

Using cytosolic and organelle-targeted Aeq, we have previously demonstrated that expression of various PSs, especially the PS2 variants, reduces the steady-state free Ca^{2+} concentration of the endoplasmic reticulum ($[Ca^{2+}]_{ER}$) and Golgi apparatus ($[Ca^{2+}]_{GA}$), the major intracellular Ca^{2+} stores of mammalian cells [18]. For those experiments, we used primarily HeLa cells, a convenient and extensively used cell model. In the work here presented, we carried out the same type of measurements in two other cell types, the SH-SY5Y cell line, derived from a human neuroblastoma, and mouse embryonic fibroblasts (MEFs). The latter cell model offers the possibility that a PS double knockout (DKO) clone is also available [31].

SH-SY5Y cells were cotransfected with the cDNAs coding for a recombinant Aeq targeted to the endoplasmic reticulum (ER-Aeq) and for PS2-T122R, a FAD-linked mutant PS2 whose effect at the Ca^{2+} store level was originally described in human FAD fibroblasts and HeLa cells [18, 21]; control cells were transfected with ER-Aeq and vector alone (pcDNA3). Twenty-four to 48 hrs after transfection, Ca^{2+} stores were depleted in a Ca^{2+}-free, EGTA-containing medium to allow ER-Aeq reconstitution (see Materials and Methods) and subsequently the refilling process was continuously monitored upon addition of $CaCl_2$ (1 mM) to the bathing medium. Under these conditions, the $[Ca^{2+}]_{ER}$ increased in a couple of minutes up to a plateau that stabilized at a significant lower level in PS2−T122R–expressing cells, with respect to control cells (Fig. 1A). Table 1 reports the steady-state $[Ca^{2+}]_{ER}$ obtained with this protocol in all the cell types here investigated: HeLa, SH-SY5Y, wt and DKO MEFs. Note that PS2-T122R was maximally effective in SH-SY5Y cells (–53 ± 3%, mean ± S.E.M., $n = 29$).

The question then arises as to the molecular mechanisms leading to this reduced steady-state $[Ca^{2+}]_{ER}$. A first possibility is that it is due to an increased Ca^{2+} leak out of the stores. The passive ER Ca^{2+} leak rate was thus measured directly using a previously described procedure [32]. Briefly, cells, cotransfected with the cDNAs coding for ER-Aeq and PS2-T122R (or the void vector), were first allowed to refill their emptied stores until they reached a steady-state. In the typical experiment with SH−SY5Y cells, shown in Fig. 1B, a wide range of external Ca^{2+} concentrations (0.125–0.25–0.5–1 mM) was used in order to obtain different levels of the steady-state $[Ca^{2+}]_{ER}$ before leak measurement; typically, three cover slips, for both control and mutant PS2–expressing cells, were used at each Ca^{2+} concentration. At the plateau, the SERCA inhibitor cyclopiazonic acid, CPA (20 μM), was added in a Ca^{2+}-free medium containing EGTA (1 mM) to remove extracellular Ca^{2+} and the rate of $[Ca^{2+}]_{ER}$ decay was continuously monitored (Fig. 1A and B). The single traces were averaged and aligned to CPA addition (grey and black traces for control and PS2-T122R–expressing cells, respectively). Figure 1C shows the average rate of Ca^{2+} leakage ($-d[Ca^{2+}]_{ER}/dt$) as a function of the instantaneous $[Ca^{2+}]_{ER}$, estimated from the traces shown in Fig. 1B (grey and black symbols, for control and PS2-T122R–expressing cells, respectively). In cells expressing the mutant PS2, at $[Ca^{2+}]_{ER}$ above 40 μM, the decay rates are significantly higher than those of controls. The linear fit of the experimental data shown in Fig. 1C thus shows a significantly greater slope for PS2-T122R–expressing cells compared with control ones, being respectively (s^{-1}) 0.040 ± 0.003 and 0.032 ± 0.002 ($n = 24$, $P < 0.001$). The percentage increase in slope, averaged among different cell batches, was 17.1 ± 6.3% ($n = 7$). When similar experiments were carried out in HeLa cells (Fig. 1D–F), the estimated slopes were (s^{-1}) 0.031 ± 0.3, 0.035 ± 0.001, 0.031 ± 0.004 and 0.028 ± 0.003 for cells transfected, respectively, with the cDNA coding for PS2-T122R, PS2-M239I, wt PS2 and the void vector. Compared with SH−SY5Y cells, expression of PS2-T122R in HeLa cells resulted in a smaller increase in slope (9.1 ± 2.3%, $n = 3$) (see also Table 1 and [18]).

It has to be mentioned that in control, void-vector transfected SH-SY5Y and HeLa cells (Figs 1C–F), the absolute values of the decay rates were rather similar for the same ER Ca^{2+} level, that is, around 2.8−3 μM/sec. at 100 μM $[Ca^{2+}]_{ER}$ for the two cell types. Indeed, in control cells, ER leak rates covered higher ranges in

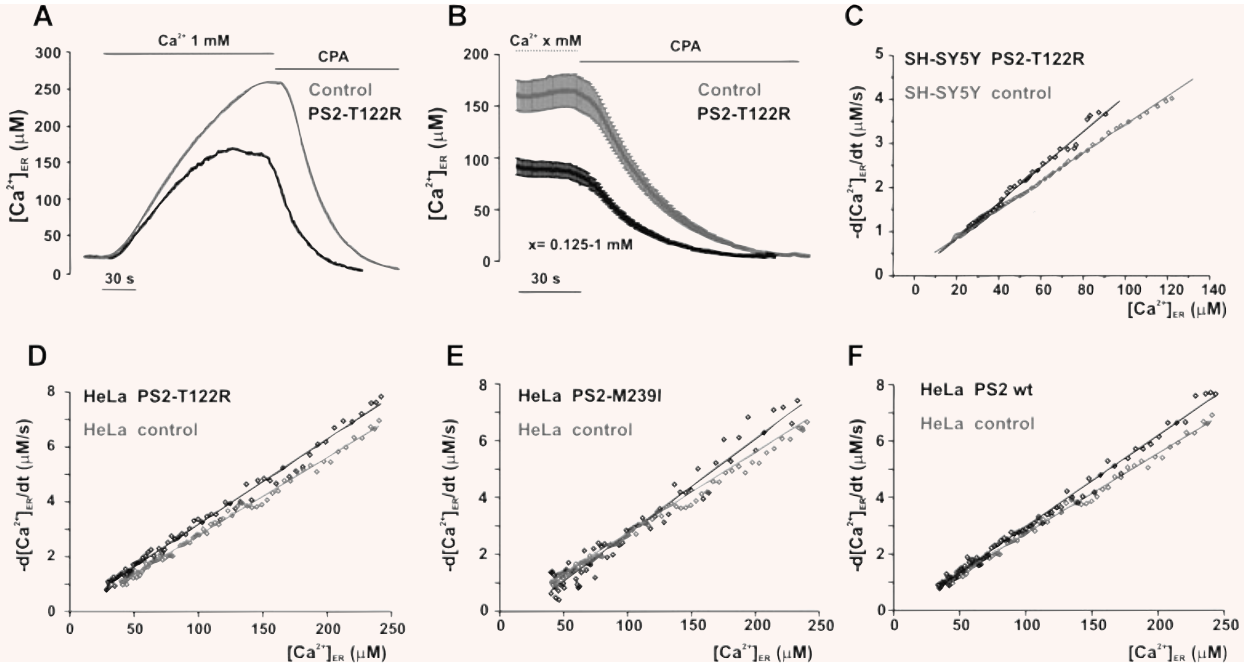

Fig. 1 Effect of PS2 variants on passive ER Ca^{2+} leak. (**A**) Representative traces of $[Ca^{2+}]_{ER}$ measurements in SH-SY5Y cells transiently cotransfected with the cDNAs coding for ER-Aeq and PS2-T122R (black) or with the void vector as control (grey). After Aeq reconstitution (see Materials and Methods), cells were washed and bathed in a Ca^{2+}-free, EGTA (0.6 mM)-containing medium before exposure to $CaCl_2$ (1 mM). The passive ER Ca^{2+} leak was estimated by addition, at the plateau, of CPA (20 μM) together with EGTA (1 mM). (**B**) For quantitative analysis of ER Ca^{2+} leak, different steady-states of $[Ca^{2+}]_{ER}$ were obtained by the addition of $CaCl_2$ ranging from 0.125 to 1 mM. The single traces were averaged and aligned to CPA addition (grey and black traces for control and PS2-T122R–expressing cells, respectively, mean ± S.E.M., $n = 24$). (**C**) The rate of ER Ca^{2+} loss ($-d[Ca^{2+}]/dt$) was plotted as a function of the instantaneous $[Ca^{2+}]_{ER}$ estimated from single traces as shown in (**B**) (black and grey symbols, for PS2-T122R-expressing and control cells, respectively). The S.E.M. was omitted for clarity. (**D**–**F**) Experiments with HeLa cells were carried out as described in (**A**) and analysed as shown in (**B**) and (**C**) (black and grey symbols for PS2-expressing and control cells, respectively, $n = 6$–9).

Table 1 ER Ca^{2+} levels (μM)

Cell type	Control	*n*	PS2-T122R	*n*	% change
HeLa	414.4 ± 12.8	54	336.1 ± 11.5*	30	−19
SH-SY5Y	298.2 ± 9.6	28	140.5 ± 8.0***	29	−53
wt MEFs	310.7 ± 27.0	27	180.0 ± 21.8***	9	−42
DKO MEFs	306.5 ± 27.4	11	211.6 ± 16.1***	10	−31

*$P < 0.05$, **$P < 0.01$, ***$P < 0.001$.

HeLa (0−12 μM/sec.) than in SH-SY5Y (0−6 μM/sec.) being the latter cell type characterized by a lower maximal steady-state ER Ca^{2+} level (see Table 1).

The rate of $[Ca^{2+}]_{ER}$ decay in intact cells can be influenced by factors other than the intrinsic ER Ca^{2+} leak, for example, the rate of Ca^{2+} extrusion across the plasma membrane or the rate of Ca^{2+} sequestration by mitochondria or other organelles. We thus investigated whether the reduction of the steady-state ER Ca^{2+} level, induced by transient expression of mutant PS2, could also be observed in digitonin permeabilized cells with the free $[Ca^{2+}]$ of the bathing solution ($[Ca^{2+}]_o$) buffered at a constant level by an EGTA-based buffer (see Materials and Methods). Under these conditions, SH−SY5Y cells cotransfected with the cDNAs coding for ER-Aeq and PS2-T122R showed a reduction of the $[Ca^{2+}]_{ER}$ (compared with controls) similar to that found in intact cells: 53 and 47%, respectively, in intact and permeabilized SH−SY5Y cells (Fig. 2A). Similar results were also obtained in DKO MEFs (Fig. 2B). The capability of PS2-T122R to reduce the $[Ca^{2+}]_{ER}$ level upon cell treatment with digitonin (20−100 μM, 1–2 min.) was confirmed also in an SH-SY5Y clone stably expressing PS2−T122R. The estimated $[Ca^{2+}]_{ER}$ reductions, compared with the void-vector transfect clone, were 25.8 ± 2.9% ($n = 20$, $P < 0.01$) and 28.1 ± 5.4% ($n = 22$, $P < 0.01$), respectively, in intact and permeabilized cells.

PS2-T122R effect on ER Ca^{2+} channels

It has been suggested that, in PC12 cells and in cortical neurons, PS2-N141I (as well as PS1 mutations) alters Ca^{2+} homeostasis

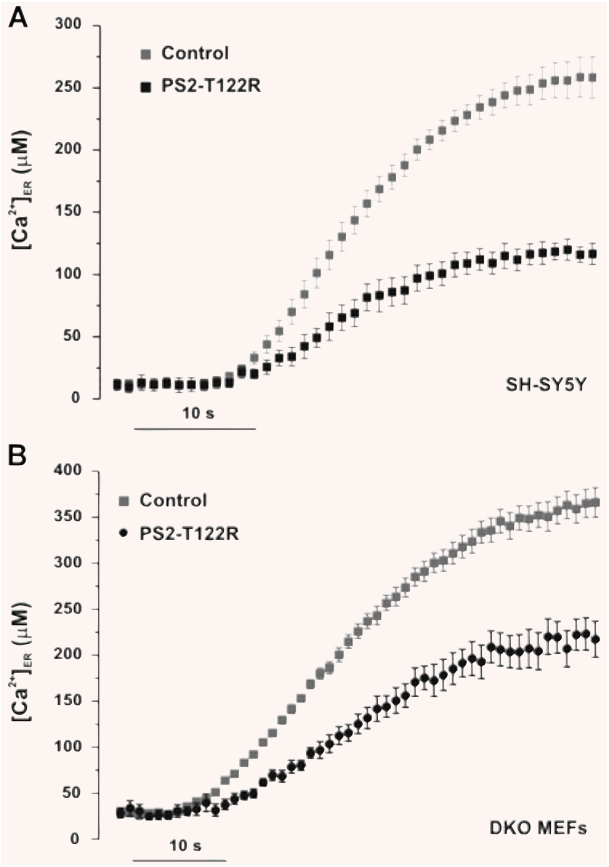

Fig. 2 Effect of PS2-T122R on ER Ca^{2+} uptake. SH-SY5Y cells (**A**) and DKO MEFs (**B**) were transiently cotransfected with the cDNAs coding for ER-Aeq and PS2-T122R (black) or with the void vector as control (grey). Upon Aeq reconstitution (see Materials and Methods), the cells were washed and bathed in a Ca^{2+}-free, EGTA (0.6 mM)-containing medium. The cells were then permeabilized for 2 min. with digitonin (20 μM) in an EGTA-containing intracellular solution. Upon washing, ER Ca^{2+} uptake was followed in the same solution containing an EGTA-based buffer (free $[Ca^{2+}] = 0.3$ μM) and ATP (0.2 mM) (see Materials and Methods). Traces were aligned to Ca^{2+} addition, black and grey symbols for PS2-T122R expressing and control cells, respectively (mean ± S.E.M., $n = 12$ for SH-SY5Y and $n = 16$ for DKO MEFs).

by interfering with ryanodine receptors (RyRs) [2, 9, 10]. Furthermore, it has been shown that, in triple transgenic mice, the knock-in of PS1-M146V up-regulates the expression of RyRs in the brain [5, 13] and in single-channel activity experiments, the cytosolic N-terminus of PS1 or PS2 potentiates mouse RyR open probability [33, 34]. We employed a pharmacological approach to investigate whether RyRs could be possibly involved in the effect of PS2-T122R on ER Ca^{2+} handling. In intact SH-SY5Y cells, an overnight treatment with the classical RyR inhibitor dantrolene (20 μM) caused only a minor reduction of the PS2-T122R effect. In fact, when the Ca^{2+} store content was estimated by cyt-Aeq following the addition of CPA (20 μM) plus bradykinin (Bk, 100 nM) (Fig. 3A), a small but significant recovery of the reduction caused by PS2-T122R was observed (+12%, $P < 0.05$) (Fig. 3B). A similar trend to a recovery, albeit not statistically significant (+5%), was found while monitoring the steady-state ER Ca^{2+} level in dantrolene−treated cells (data not shown). Consistently with the modest effect found upon RyR inhibition, the process of Ca^{2+}-induced Ca^{2+} release seemed not to play a dominant role, since in permeabilized SH-SY5Y cells perfused with an intracellular solution containing BAPTA (a Ca^{2+} chelator acting faster than EGTA) the effect of PS2-T122R on the $[Ca^{2+}]_{ER}$ was similar, being the estimated reductions of ER Ca^{2+} plateaus 39 ± 3% and 34 ± 3% (mean ± S.E.M., $n = 3$), respectively, with BAPTA- and EGTA-based buffers (see Materials and Methods).

IP_3Rs are the other class of Ca^{2+} release channels that have also been involved in the modulation of Ca^{2+} handling by PSs [4, 7, 11, 12, 22]. When the steady-state $[Ca^{2+}]_{ER}$ was monitored in permeabilized SH-SY5Y cells, transfected with ER-Aeq and PS2-T122R, addition of the IP_3R antagonist heparin (100–200 μg/ml) had no effect or caused only a marginal recovery. On average, the reduction in the steady-state was maintained (40 ± 1.4% and 41 ± 6%, mean ± S.E.M., $n = 5$, respectively, with and without heparin). The other IP_3R inhibitor 2−aminoethoxydiphenyl borate (2−APB) could not be used because it interfered with the ER-Aeq–based detection system already at 20 μM, a concentration smaller than that usually employed to block the receptor (unpublished data). In MEFs that, at variance with SH-SY5Y, express high levels of IP_3R-3 in addition to IP_3R-1 [22, 35], knocking down IP_3R-3 by a specific siRNA, partially rescued (+10%, $P < 0.01$) the ER Ca^{2+} defect caused by expression of PS2-T122R in the same interfered cells (Fig. 3C); a siRNA specific for the type 1 IP_3R was ineffective (Fig. 3D). Although siRNAs to both IP_3Rs significantly and potently reduced the specific receptor level, no additional rescue was found (data not shown).

We also investigated another possible ER exit pathway for Ca^{2+} ions. It has recently been suggested that the protein import machinery across the ER membrane could be a relevant $Ca^{2+}{}_0$ leak pathway. In particular, it has been shown that the protein import machinery, the so-called ribosomal–translocon complex (RTC), once freed of the newly synthesized protein, can allow the flux of Ca^{2+} ions and small sugars [36–38].

When SH-SY5Y cells were maintained in the presence of puromycin (200 μM), following a 10-min. pre-incubation at 37°C, a protocol sufficient to release nascent proteins and leave the RTC in an open configuration [36], the steady-state $[Ca^{2+}]_{ER}$ was unaffected both in control and PS2-T122R–expressing cells (Fig. 4A). When a similar treatment was also employed in control SH-SY5Y cells expressing cyt-Aeq, the rate of store Ca^{2+} efflux ($d[Ca^{2+}]_{cyt}/dt$) induced by CPA addition was of the same magnitude with or without puromycin treatment (9.6 ± 0.5 nM/sec. and 8.9 ± 1.0 nM/sec., mean ± S.E.M., $n = 3$). The involvement of the RTC as a possible target of PS action was also investigated by employing anisomycin. This peptidyl-transferase inhibitor locks

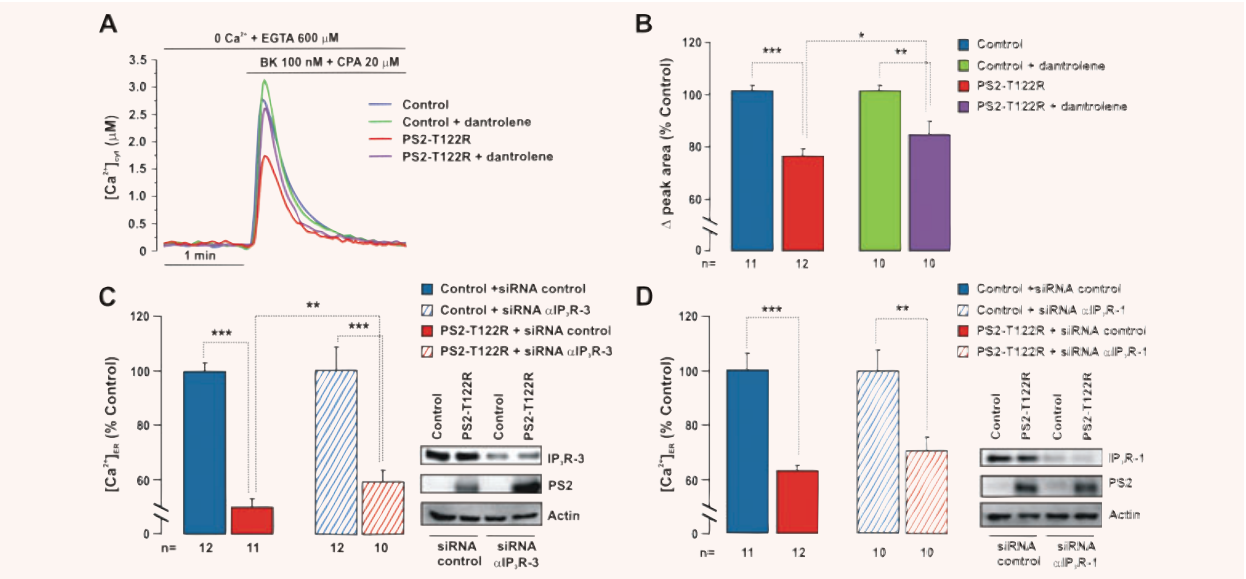

Fig. 3 Role of RyRs and IP_3Rs. (**A**) SH-SY5Y cells, transiently cotransfected with the cDNAs coding for cyt-Aeq and PS2-T122R (red trace), or with the void vector, control (blue trace), were overnight treated with dantrolene (20 μM) and continuously maintained in the presence of the drug (purple and green traces, respectively). Upon Aeq reconstitution (see Materials and Methods), the cells were washed in mKRB and then exposed to CPA (20 μM) plus bradykinin (Bk, 100 nM) in a Ca^{2+}-free, EGTA (0.6 mM)-containing medium to fully discharge the intracellular Ca^{2+} stores. (**B**) Bars represent the average peak area measured above the baseline and expressed as percentage of control, void-vector transfected cells (mean ± S.E.M.). (**C**, **D**) wt MEFs were cotransfected with the cDNAs coding for ER-Aeq and PS2-T122R (or with the void vector as control) and siRNA specific for mouse IP_3R-3 (40 nM) (**C**), IP_3R-1 (20 nM) (**D**) or equivalent amounts of control siRNA (**C**, **D**). After 48 hrs, cells were harvested and probed for expression levels of PS2 and IP_3Rs by Western blotting (right) or were employed to measure steady-state ER Ca^{2+} levels (left), according to the protocol described in Fig. 1A. Bars represent the average $[Ca^{2+}]_{ER}$ expressed as percentage of control cells transfected with the void-vector and control siRNA (mean ± S.E.M.). Note interruption in the *Y* axes in (**B–D**).

Fig. 4 Role of the ribosomal–translocon complex. (**A**) SH-SY5Y cells were transiently cotransfected with the cDNAs coding for ER-Aeq and PS2-T122R (or with the void vector as control). Upon ER-Aeq reconstitution, cells were treated for 10 min. with puromycin (0.2 mM) at 37°C and continuously maintained in the presence of the drug. ER Ca^{2+} levels were measured as described in Fig. 1A. (**B**) SH-SY5Y cells were transfected as described in (**A**). Anisomycin (0.2 mM) was present during ER-Aeq reconstitution and throughout the experiments. Bars represent the average $[Ca^{2+}]_{ER}$ (μM) (mean ± S.E.M.).

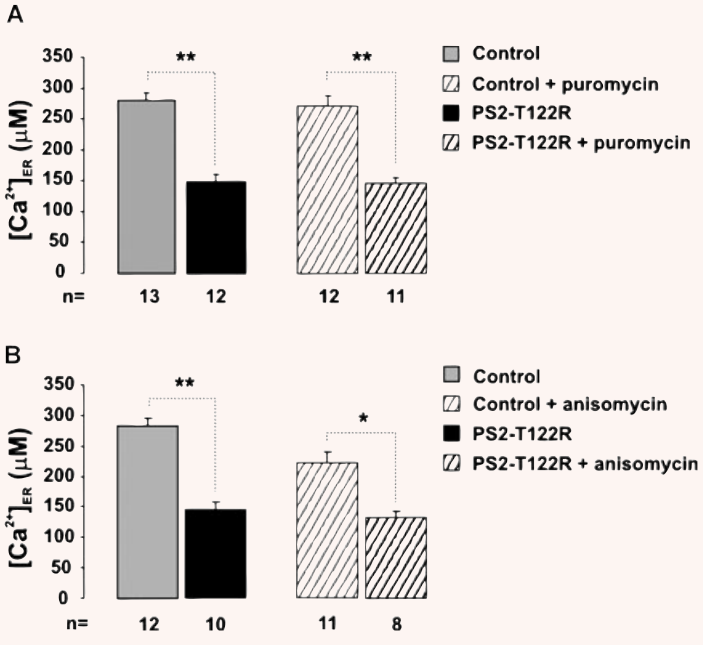

nascent chains in the ribosome, leaving the RTC in a closed configuration. Anisomycin was reported to prevent opening of the RTC if added simultaneously or before puromycin [36]. As shown in Fig. 4B, incubation for 1 hr at 4°C with anisomycin (200 μM) during the ER-Aeq reconstitution protocol, and continuous exposure to the drug during the experiment, did not prevent the reduction of the ER Ca^{2+} level, induced by PS2-T122R expression in SH-SY5Y cells. Interestingly, treatment with this drug, that should close a passive ER Ca^{2+} leak pathway, decreased the steady-state ER Ca^{2+} level in the control cells (–22 ± 6.8%, $n = 6$, $P < 0.05$).

Based on indirect evidence, that is, cytosolic Ca^{2+} sequestration, LaFerla and colleagues recently suggested that wt PS1 and PS2, as well as an FAD mutant PS1 (M146V), increase SERCA activity [25]. To directly address whether and how PS2 affects the activity of SERCA pumps, we carried out a detailed analysis in permeabilized SH−SY5Y cells by means of ER-Aeq. Ca^{2+} uptake rates were measured in different ranges of free $[Ca^{2+}]_o$, set by distinct Ca^{2+}-EGTA–based buffers (see Materials and Methods). The maximal values of the first derivative of the instantaneous $[Ca^{2+}]_{ER}$ ($d[Ca^{2+}]_{ER}/dt$) were plotted as a function of the imposed free $[Ca^{2+}]_o$ (Fig. 5A). Expression of PS2-T122R significantly and consistently reduced the maximal rate of Ca^{2+} uptake, at all the $[Ca^{2+}]_o$ tested. Similar reductions in ER Ca^{2+} uptake were observed in DKO MEFs (Fig. 5B) and wt MEFs (data not shown) expressing PS2-T122R, upon cell permeabilization with digitonin (20 μM). Table 2 reports the estimated K_m and V_{max} values of Ca^{2+} uptake obtained by double-reciprocal plots; in all cell types, the trend was similar: expression of PS2-T122R strongly reduced the V_{max} (22–35%) with modest increases in the K_m (7–16%). Noteworthy, in DKO MEFs, the ER Ca^{2+} uptake rates were also similarly reduced upon expression of wt PS2 (12.2 ± 0.9 μM/sec. and 9.4 ± 0.9 μM/sec., for control and wt PS2–expressing cells with the free $[Ca^{2+}]$ buffered at 300 nM; mean ± S.E.M., $n = 7$, $P < 0.05$; Fig. 5B, triangles). It should be stressed that these values represent the initial rates of the Ca^{2+} refilling process, that is, when the PS2 effect on leak rates should be negligible, being the ER lumen practically empty of Ca^{2+}. Differences in maximal uptake rates were maintained even in the presence of heparin (200 μg/ml; data not shown).

Because expression of PS2-T122R reduces the ER Ca^{2+} uptake without reducing the SERCA-2 protein level (Fig. 5C), the simplest interpretation of these results is that PS2 variants affect directly or indirectly the activity of the pump. Experiments were carried out to determine whether the ER Ca^{2+} depletion induced by PS2-T122R could be compensated by increasing the number of SERCA-2B. Figure 5D and E shows the results obtained by monitoring ER Ca^{2+} levels in digitonin permeabilized SH-SY5Y cells: over-expression of SERCA-2B together with PS2-T122R allowed to fully recover both the maximal uptake rate and the ER Ca^{2+} plateau found in control cells.

Conformation of PS2 and store Ca^{2+} handling

It has been reported that only the full-length (FL), immature forms of wt PSs (but not FAD-linked mutants) can form ER Ca^{2+} leak channels [23, 26] (but see also [11]). We asked which form of the protein, the FL or the dimeric complex formed by the N- and C-terminal fragments (NTF, CTF), is responsible for the reduced ER Ca^{2+} level here reported. In DKO MEFs, transient expression of the loss-of-function mutant PS2-D366A, which is devoid of γ-secretase as well as presenilinase activity [39] (Fig. 6A), reduced the ER Ca^{2+} level by an amount similar to that observed upon expression of wt or mutant PS2 (Fig. 6B).

Lendahl and colleagues [40] have previously demonstrated that, in DB8 cells KO for both PSs, co-expression of the NTF and CTF of wt PS2, by means of a bicistronic vector, allows the recovery of γ-secretase activity. We confirmed this result in DKO MEFs by employing a recently developed γ-secretase cell assay [30] (Fig. 6C); NTF and CTF co-expression, however, failed to mimic the effect of wt or mutant PS2 on Ca^{2+} handling (Fig. 6B).

Role of endogenous PS2 on ER Ca^{2+} uptake

All the above results were obtained in cells over-expressing PS2. To test whether physiological PS2 levels play a role in ER Ca^{2+} handling, wt MEFs were cotransfected with siRNA specific for mouse PS2 and the cDNA coding for ER-Aeq. As shown in Fig. 7, the protein level was reduced by 50–80%, 24–48 hrs after transfection (see Materials and Methods). When ER Ca^{2+} plateaus and uptake rates were evaluated, upon digitonin permeabilization, a small but significant increase in both parameters was detected in cells knocked down for PS2, compared with cells treated with control siRNA (Fig. 7A and B). On the other hand, when cells were transfected with the cDNA coding for ubiquilin1 [41] (Fig. 7C) or were treated overnight with the presenilinase inhibitor MW167 (15 μM) [42] (Fig. 7D), both treatments known to increase FL PS levels by interfering with PS processing, significant decreases of ER Ca^{2+} plateaus were observed in wt but not in DKO MEFs.

We had previously shown that, in HeLa and SH-SY5Y cells as well as in human FAD fibroblasts, PS1 mutants partially mimicked the ER Ca^{2+}–depleting effect of PS2 mutants [18]. We here evaluated the hypothesis that the former mutants can exert an ER-depleting effect only in the presence of PS, that is, in an endogenous PS background. In fact, the transient expression of PS1-A246E significantly decreased the ER Ca^{2+} plateau by 25% in wt MEFs (243 ± 34 μM and 325 ± 21 μM, mean ± S.E.M., $P < 0.05$, $n = 9$) but not in DKO MEFs (270 ± 28 μM and 314 ± 20 μM, mean ± S.E.M., $n = 9$; Fig. 7E).

Discussion

We have previously reported that different FAD-linked PS1 and PS2 mutants instead of causing a Ca^{2+} overload, *reduce* the ER Ca^{2+} content in different model cells, including fibroblasts from FAD patients and rat primary neurons. The effect is consistent and more dramatic with PS2 variants, and it is also mimicked by

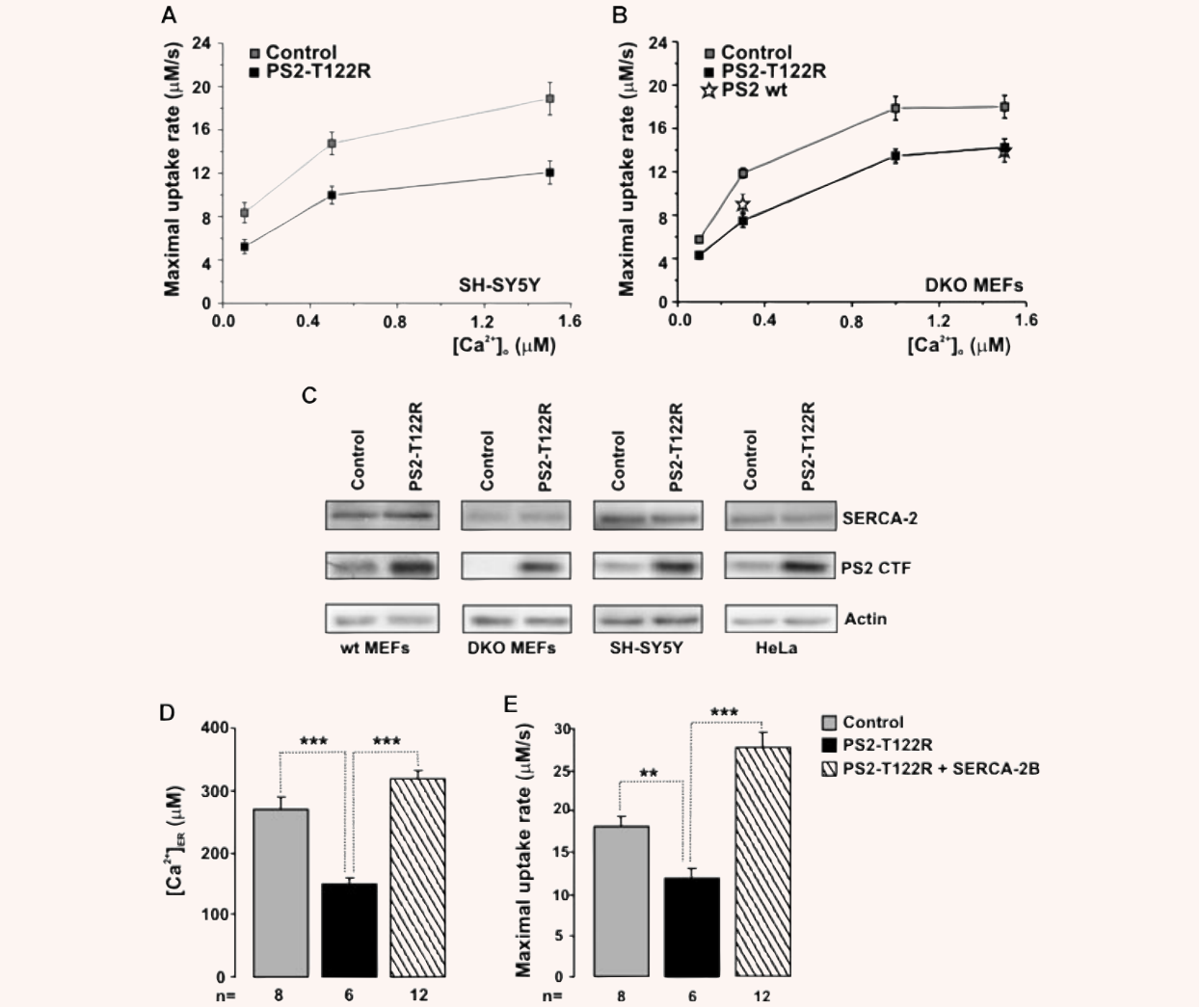

Fig. 5 Effect of PS2-T122R on ER Ca^{2+} uptake. (**A**, **B**) ER Ca^{2+} uptake was followed in permeabilized SH-SY5Y cells and DKO MEFs at different free $[Ca^{2+}]_o$ as described in Fig. 2. The maximal values of the first derivative of the instantaneous $[Ca^{2+}]_{ER}$ ($d[Ca^{2+}]_{ER}/dt$) were plotted as a function of the free external $[Ca^{2+}]_o$ (mean ± S.E.M., *n* ranging from 6 to 20). (**B**) also shows the values obtained with PS2 wt (empty stars): 9.4 ± 0.9 μM/sec. ($n = 7$) and 14.4 ± 0.8 μM/sec. ($n = 8$), respectively, at 0.3 and 1.5 μM $[Ca^{2+}]_o$. (**C**) Western blots showing SERCA-2 and PS2 levels in control and PS2-T122R–expressing cell lines. (**D**, **E**) SH-SY5Y cells were transiently cotransfected with the cDNAs coding for ER-Aeq and PS2-T122R in the absence (black bars) or presence of SERCA-2B cDNA (hatched bars); control cells were cotransfected with ER-Aeq cDNA and with the void vector (grey). Bars represent the average $[Ca^{2+}]_{ER}$ (μM) (**D**) and maximal uptake rates (μM/sec.) (**E**) (mean ± S.E.M.).

Table 2 Kinetic parameters of ER Ca^{2+} uptake

	K_m (nM)		% change	V_{max} (μM/sec.)		% change
Cell type	**Control**	**PS2-T122R**		**Control**	**PS2-T122R**	
SH-SY5Y	150	167	11	19.3	12.8	−34
wt MEFs	164	175	7	14.5	10.1	−30
DKO MEFs	277	321	16	21	16.4	−22

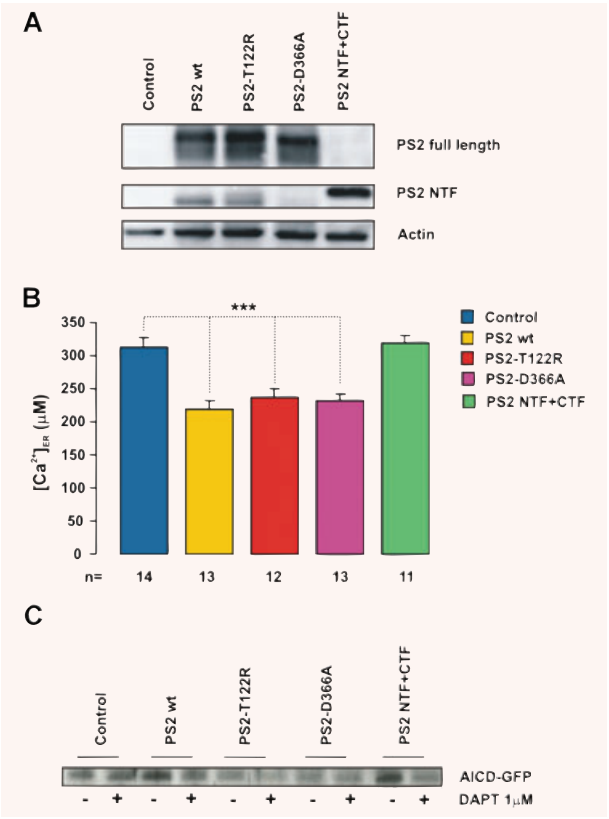

Fig. 6 Effect of PS2 conformation on ER Ca^{2+} levels. (**A**) DKO MEFs were cotransfected with the cDNA coding for ER-Aeq and a PS2 variant (wt, T122R or D366A) or with a bicistronic vector coding for the NTF and CTF of wt PS2. The Western blot shows the expression level of PS2 (FL and NTF). The PS2 NTF of cells transfected with the bicistronic vector migrates at higher MW because of a myc-tag. (**B**) Bars represent the average $[Ca^{2+}]_{ER}$ (μM) for DKO MEFs described in (**A**) (mean ± S.E.M.). (**C**) The γ-secretase activity was checked in DKO-MEFs transfected with the cDNA coding for C99-GFP as suitable substrate. Co-expression of wt PS2, PS2-T122R or PS2 NTF+CTF, but not PS2-D366A, led to AICD-GFP generation, as detected by Western blot with an anti-GFP antibody. For each condition, cells were also overnight treated with DAPT (1 μM).

over-expression of wt PS2 [18, 20, 21]. Similar conclusions have also been reached in neuroblastoma cells by over-expression of the wt forms of PS2 and PS1 [19]. Mild reductions of store Ca^{2+} levels rather than Ca^{2+} overloads were also recently reported in DT40 cells expressing PS1−M146L [11]. Taken together, these data, while questioning the 'Ca^{2+} overload' hypothesis [15, 43], strongly suggest that PSs might be key determinants in setting the ER Ca^{2+} level. We here investigated the molecular mechanism by which wt and mutant PS2 reduce the ER Ca^{2+} content of intracellular stores. To this aim, in addition to HeLa cells, we also used neuroblastoma SH-SY5Y cells and two MEFs clones, with and without endogenous PSs (wt and DKO MEFs, respectively).

When the effect of the transient expression of PS2-T122R was taken as a reference to compare the different cell types, we invariably observed a reduction in the steady-state $[Ca^{2+}]_{ER}$, ranging from about 50% to 20%, with the following efficacy order: SH-SY5Y > wt MEFs ≥ DKO MEFs > HeLa cells. All these models were thus employed to untangle the likely common mechanisms that underlie the PS2 effect.

By means of ER-Aeq, we initially verified whether the amount of passive ER Ca^{2+} leak was increased by expression of wt and mutant PS2. In the absence of Ca^{2+} and in the presence of a SERCA inhibitor, the decay rate of the $[Ca^{2+}]_{ER}$ was modestly but significantly accelerated by expression of PS2-T122R. The effect was more pronounced in SH-SY5Y (+17%) than HeLa cells (+9%). Of note, an increased leakage was also found upon expression of PS2-M239I or wt PS2.

Passive ER leak may be accounted for by classical Ca^{2+} release channels. Indeed, PS2 has been suggested to increase number and/or sensitivity of both RyRs [9, 10, 34, 44] and IP_3Rs [7, 11, 12, 22]. In SH-SY5Y and wt MEF cells, where the PS2 effect was more pronounced, pharmacological (dantrolene and heparin) and genetic (siRNA) approaches, allowed us to estimate an increase in leak, due to both RyRs and IP_3Rs (type 3), that corresponds to about 15%, a value not far from that found in HeLa and SH-SY5Y cells by measuring passive ER Ca^{2+} leakage in the presence of CPA (ranging from 9% to 17%).

We also verified that PS2 did not exert its effect by acting on the protein import machinery, the so-called RTC, which was recently suggested to represent a relevant ER Ca^{2+} efflux pathway [36–38]. Puromycin, a known RTC opener [36], was not able to mimic the PS2 effect on both the cytosolic and ER Ca^{2+} levels of SH-SY5Y cells. Notably, puromycin by itself did not increase the rate of Ca^{2+} exit from the stores. In contrast, anisomycin, a drug that should keep the RTC closed, did not rescue the ER Ca^{2+} loss caused by mutant PS2. Taken together, these data indicate that, at least in SH-SY5Y cells, the RTC does not significantly contribute to the resting ER Ca^{2+} leakage or to that induced by expressed PS2.

We also verified whether there was an effect of PS on ER Ca^{2+} uptake. In intact cells, uptake rates do not simply reflect pump activity, as they are also affected by Ca^{2+} influx/extrusion processes across the plasma membrane and mitochondria Ca^{2+} buffering. To overcome these uncertainties, studies were thus carried out in digitonin permeabilized cells with the free $[Ca^{2+}]$ of the bathing medium buffered at different values (0.1–2 μM). At these Ca^{2+} concentrations, the contribution of mitochondria to Ca^{2+} uptake is negligible. Under these conditions, in cells expressing PS2-T122R, reductions of Ca^{2+} uptake rates were found at each Ca^{2+} concentration tested. Similar results were also obtained in DKO MEFs expressing wt PS2. In SH-SY5Y, over-expression of SERCA-2B together with PS2-T122R rescued both ER Ca^{2+} uptake rates and steady-state levels at, or above, the values observed in control, void-vector transfected cells. Recently, Green *et al.* [25] have shown that wt PS1 and PS2 as well as an FAD-linked mutant (PS1-M146V) increase SERCA-2 activity. Those data, however, have been obtained by monitoring cytosolic Ca^{2+} clearance in intact *Xenopus* oocytes, that is, under conditions

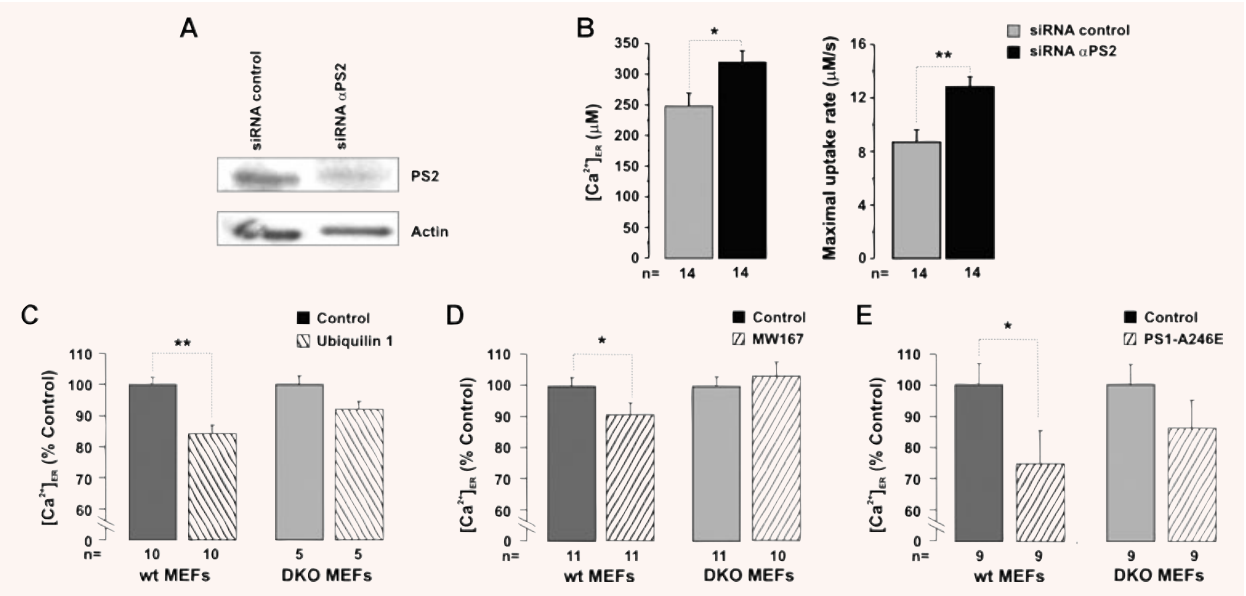

Fig. 7 Effect of endogenous PS2 on ER Ca^{2+} uptake. (**A**) wt MEFs were transfected with the cDNA coding for ER-Aeq and siRNA specific for mouse PS2 or control siRNA (20 nM). After 48 hrs, part of the cells was harvested to check the expression level of PS2 by Western blotting. (**B**) The same cells were used to estimate ER Ca^{2+} uptake upon cell permeabilization with the protocol described in Fig. 2. Bars represent the average $[Ca^{2+}]_{ER}$ (μM) (left) and maximal uptake rates (μM/sec.) (right) (mean ± S.E.M.). (**C**) wt and DKO MEFs were transfected with the cDNA coding for ER-Aeq and ubiquilin1. (**D**) wt and DKO MEFs were transfected with the cDNA coding for ER-Aeq and overnight treated with MW167 (15 μM) or vehicle (DMSO). (**E**) wt and DKO MEFs were transfected with the cDNA coding for ER-Aeq and PS1-A246E or its void vector (control). Bars represent the average $[Ca^{2+}]_{ER}$ (mean ± S.E.M.) expressed as percentage of control cells transfected with the void vector (**C**, **E**) or treated with vehicle (**D**); note interruption in the *Y* axes. (**C**–**E**) Upon Aeq reconstitution, steady-state ER levels were measured as described in Fig. 1A.

where other factors such as the amplitude of capacitative Ca^{2+} influx, the activity of the plasma membrane Ca^{2+} ATPase and the contribution of mitochondrial Ca^{2+} uptake may complicate data interpretation. From our results obtained in permeabilized cells, we could conclude that PS2-T122R affects the maximal capacity of the pump rather than its K_m, which appears to be set around 0.15–0.3 μM, a value not far from that reported for purified SERCA-2B (0.17 μM) [45].

With these results in mind, one would expect to find ER Ca^{2+} overloads in DKO MEFs, if compared with wt MEFs. On the contrary, we found similar ER Ca^{2+} steady-state levels and about a 20% increase in ER Ca^{2+} uptake rates in permeabilized DKO MEFs. It should be noted that previous data using these model cells found both ER Ca^{2+} overload [23] and ER Ca^{2+} reduction [22, 25], despite the fact that these clones all derive from the same laboratory (B. De Strooper's lab; [31]). The different results do not depend on different approaches to test Ca^{2+} handling, since both the fura-2 [23, 25] and recombinant aequorin [22] were used, as we did. Moreover, we could not confirm in the DKO MEFs differences in the expression levels of IP_3Rs [22] or SERCAs [25]. These discrepancies indicate that, despite originating from the same transgenic mice, cell clones can substantially differ one from the other (at least in terms of Ca^{2+} handling) and, more important, that a cause–effect relationship between alterations in Ca^{2+} homeostatic machinery and lack of PS expression cannot be unambiguously established using these cells. On the contrary, such a cause–effect relationship appears more easily and consistently found upon transient expression of wt or mutant PS1/2 in each clone. We followed this approach to test the hypothesis that endogenous PS2 works as a brake on ER Ca^{2+} uptake. Along the same line, in wt MEFs, knocking down the endogenous level of PS2 by siRNAs increased both ER Ca^{2+} pumping and steady-state levels, thus unmasking the inhibitory role played by PS2.

In DKO MEFs, the effect of mutant PS2 on ER Ca^{2+} handling does not qualitatively differ from that exerted by either wt PS2 or PS2-D366A, a loss-of-function, non-pathogenic mutant also devoid of presenilinase activity (see Fig. 6A and [39]). These findings suggest that PS2 and possibly SERCA-2 interact independently of the γ-secretase activity and the intra-molecular cut of PS2. To further address this issue, we have co-expressed the NTF and CTF of wt PS2 in DKO MEFs using a bicistronic vector [40]. Expression of the two separate fragments, while being able to rescue the γ-secretase activity, was unable to mimic the effect of PS2 on ER Ca^{2+} handling. Furthermore, the Ca^{2+}-depleting effect of PS2 over-expression could be partially mimicked by ubiquilin1 over-expression [41] or inhibition of presenilinase activity by

MW167 [42], two treatments that have been previously suggested to stabilize the FL form of endogenous PS2.

We previously found that transient or stable expression of some FAD-linked PS1 mutants also causes ER Ca^{2+} depletion. This effect, however, is quantitatively much smaller than that caused by PS2 expression and is dependent on the type of mutation (A246E, M146L, P117L but not L286V; [18]) and the cell system employed. For example, PS1-A246E was effective in HeLa cells and wt MEFs but not in SH-SY5Y cells and primary rat neurons (this work and [18]). These results might be explained taking into account recent findings that suggest the capability of PS1 mutants to shift the balance from PS1 to PS2 containing γ-secretase complexes [46]. Thus, given the inhibitory role played by endogenous PS2 on ER Ca^{2+} uptake, the store-depleting effect of some PS1 mutants could be indirect and reside in their capability to potentiate the effect of endogenous PS2, either as single molecule or as part of a complex. This is, however, only a working hypothesis, and additional experiments are required to address this specific point.

In conclusion, we here provide evidence showing that PS2 has a dual role on ER Ca^{2+} homeostasis: (*i*) it inhibits SERCAs and (*ii*) increases Ca^{2+} leak through ER Ca^{2+} channels (RyRs and IP_3R-3). The effect on Ca^{2+} uptake was dominant in SH-SY5Y with respect to HeLa cells. This finding is consistent with the fact that cells of the former type, like neurons, have very low resting ER Ca^{2+} levels. Altogether, these results suggest that PS2 plays a direct, primary role on Ca^{2+} handling by intracellular stores while strengthening the idea of a complex interplay between PS1 and PS2.

Acknowledgements

We thank I. Moressa. and V. Rocchetto for performing some of the experiments; G. Ronconi and M. Santato for technical assistance. This work was supported by grants from the Italian Ministry of University and Scientific Research (MURST) to C.F., P.P. and T.P.; FIRB (grant no. RBIN042Z2Y) to P.P.; the Veneto Region (Biotech 2) and the CARIPARO Foundation to T.P. We thank G. Binetti for the cDNAs coding for wild-type and mutant presenilins (PSs); B. De Strooper for wild-type and PS double knockout mouse embryonic fibroblasts; U. Lendhal for the bicistronic vector coding for PS2 N-and C-terminal fragments; M. J. Monteiro for the cDNA coding for ubiquilin1. We are grateful to P. Magalhães for useful suggestions. L. Brunello's Ph.D. fellowship is granted by the CARIPARO Foundation.

References

1. **Guo Q, Fu W, Sopher BL, *et al.*** Increased vulnerability of hippocampal neurons to excitotoxic necrosis in presenilin-1 mutant knock-in mice. *Nat Med.* 1999; 5: 101–6.
2. **Chan SL, Mayne M, Holden CP, *et al.*** Presenilin-1 mutations increase levels of ryanodine receptors and calcium release in PC12 cells and cortical neurons. *J Biol Chem.* 2000; 275: 18195–200.
3. **Schneider I, Reverse D, Dewachter I, *et al.*** Mutant presenilins disturb neuronal calcium homeostasis in the brain of transgenic mice, decreasing the threshold for excitotoxicity and facilitating long-term potentiation. *J Biol Chem.* 2001; 276: 11539–44.
4. **Stutzmann GE, Caccamo A, LaFerla FM, *et al.*** Dysregulated IP_3 signaling in cortical neurons of knock-in mice expressing an Alzheimer's-linked mutation in presenilin1 results in exaggerated Ca^{2+} signals and altered membrane excitability. *J Neurosci.* 2004; 24: 508–13.
5. **Stutzmann GE, Smith I, Caccamo A, *et al.*** Enhanced ryanodine receptor recruitment contributes to Ca^{2+} disruptions in young, adult, and aged Alzheimer's disease mice. *J Neurosci.* 2006; 26: 5180–9.
6. **Guo Q, Furukawa K, Sopher BL, *et al.*** Alzheimer's PS-1 mutation perturbs calcium homeostasis and sensitizes PC12 cells to death induced by amyloid β-peptide. *Neuroreport.* 1996; 8: 379–83.
7. **Leissring MA, Paul BA, Parker I, *et al.*** Alzheimer's presenilin-1 mutation potentiates inositol 1,4,5-trisphosphate-mediated calcium signaling in *Xenopus* oocytes. *J Neurochem.* 1999; 72: 1061–8.
8. **Popescu BO, Cedazo-Minguez A, Benedikz E, *et al.*** γ-secretase activity of presenilin 1 regulates acetylcholine muscarinic receptor-mediated signal transduction. *J Biol Chem.* 2004; 279: 6455–64.
9. **Lee SM, Lee JW, Song YS, *et al.*** Ryanodine receptor-mediated interference of neuronal cell differentiation by presenilin 2 mutation. *J Neurosci Res.* 2005; 82: 542–50.
10. **Lee SY, Hwang DY, Kim YK, *et al.*** PS2 mutation increases neuronal cell vulnerability to neurotoxicants through activation of caspase-3 by enhancing of ryanodine receptor-mediated calcium release. *FASEB J.* 2006; 20: 151–3.
11. **Cheung KH, Shineman D, Muller M, *et al.*** Mechanism of Ca^{2+} disruption in Alzheimer's disease by presenilin regulation of InsP3 receptor channel gating. *Neuron.* 2008; 58: 871–83.
12. **Leissring MA, Parker I, LaFerla FM.** Presenilin-2 mutations modulate amplitude and kinetics of inositol 1, 4,5-trisphosphate-mediated calcium signals. *J Biol Chem.* 1999; 274: 32535–8.
13. **Smith IF, Green KN, LaFerla FM.** Calcium dysregulation in Alzheimer's disease: recent advances gained from genetically modified animals. *Cell Calcium.* 2005; 38: 427–37.
14. **Leissring MA, LaFerla FM, Callamaras N, *et al.*** Subcellular mechanisms of presenilin-mediated enhancement of calcium signaling. *Neurobiol Dis.* 2001; 8: 469–78.
15. **LaFerla FM.** Calcium dyshomeostasis and intracellular signalling in Alzheimer's disease. *Nat Rev Neurosci.* 2002; 3: 862–72.
16. **Thinakaran G, Sisodia SS.** Presenilins and Alzheimer disease: the calcium conspiracy. *Nat Neurosci.* 2006; 9: 1354–5.
17. **Lessard CB, Lussier MP, Cayouette S, *et al.*** The overexpression of presenilin2 and Alzheimer's-disease-linked presenilin2 variants influences TRPC6-enhanced Ca^{2+} entry into HEK293 cells. *Cell Signal.* 2005; 17: 437– 45.
18. **Zatti G, Burgo A, Giacomello M, *et al.*** Presenilin mutations linked to familial Alzheimer's disease reduce endoplasmic reticulum and Golgi apparatus calcium levels. *Cell Calcium.* 2006; 39: 539–50.

19. **Fedrizzi L, Lim D, Carafoli E, *et al.*** Interplay of the Ca^{2+}-binding protein dream with presenilin in neuronal Ca^{2+} signaling. *J Biol Chem.* 2008; 283: 27494–503.
20. **Zatti G, Ghidoni R, Barbiero L, *et al.*** The presenilin 2 M239I mutation associated with familial Alzheimer's disease reduces Ca^{2+} release from intracellular stores. *Neurobiol Dis.* 2004; 15: 269–78.
21. **Giacomello M, Barbiero L, Zatti G, *et al.*** Reduction of Ca^{2+} stores and capacitative Ca^{2+} entry is associated with the familial Alzheimer's disease presenilin-2 T122R mutation and anticipates the onset of dementia. *Neurobiol Dis.* 2005; 18: 638–48.
22. **Kasri NN, Kocks SL, Verbert L, *et al.*** Up-regulation of inositol 1,4,5-trisphosphate receptor type 1 is responsible for a decreased endoplasmic-reticulum Ca^{2+} content in presenilin double knock-out cells. *Cell Calcium.* 2006; 40: 41–51.
23. **Tu H, Nelson O, Bezprozvanny A, *et al.*** Presenilins form ER Ca^{2+} leak channels, a function disrupted by familial Alzheimer's disease-linked mutations. *Cell.* 2006; 126: 981–93.
24. **Yagi T, Giallourakis C, Mohanty S, *et al.*** Defective signal transduction in B lymphocytes lacking presenilin proteins. *Proc Natl Acad Sci USA.* 2008; 105: 979–84.
25. **Green KN, Demuro A, Akbari Y, *et al.*** SERCA pump activity is physiologically regulated by presenilin and regulates amyloid beta production. *J Cell Biol.* 2008; 181: 1107–16.
26. **Nelson O, Tu H, Lei T, *et al.*** Familial Alzheimer disease-linked mutations specifically disrupt Ca^{2+} leak function of presenilin 1. *J Clin Invest.* 2007; 117: 1230–9.
27. **Brini M, Marsault R, Bastianutto C, *et al.*** Transfected aequorin in the measurement of cytosolic Ca^{2+} concentration ($[Ca^{2+}]_c$): a critical evaluation. *J Biol Chem.* 1995; 270: 9896–903.
28. **Herreman A, Hartmann D, Annaert W, *et al.*** Presenilin 2 deficiency causes a mild pulmonary phenotype and no changes in amyloid precursor protein processing but enhances the embryonic lethal phenotype of presenilin 1 deficiency. *Proc Natl Acad Sci USA.* 1999; 96: 11872–7.
29. **Nyabi O, Pype S, Mercken M, *et al.*** No endogenous Aβ production in presenilin-deficient fibroblasts. *Nat Cell Biol.* 2002; 4: E164; author reply E5–6.
30. **Florean C, Zampese E, Zanese M, *et al.*** High content analysis of gamma-secretase activity reveals variable dominance of presenilin mutations linked to familial Alzheimer's disease. *Biochim Biophys Acta.* 2008; 1783: 1551–60.
31. **Herreman A, Serneels L, Annaert W, *et al.*** Total inactivation of γ-secretase activity in presenilin-deficient embryonic stem cells. *Nat Cell Biol.* 2000; 2: 461–2.
32. **Pinton P, Ferrari D, Magalhães P, *et al.*** Reduced loading of intracellular Ca^{2+} stores and downregulation of capacitative Ca^{2+} influx in Bcl-2-overexpressing cells. *J Cell Biol.* 2000; 148: 857–62.
33. **Rybalchenko V, Hwang SY, Rybalchenko N, *et al.*** The cytosolic N-terminus of presenilin-1 potentiates mouse ryanodine receptor single channel activity. *Int J Biochem Cell Biol.* 2008; 40: 84–97.
34. **Hayrapetyan V, Rybalchenko V, Rybalchenko N, *et al.*** The N-terminus of presenilin-2 increases single channel activity of brain ryanodine receptors through direct protein-protein interaction. *Cell Calcium.* 2008; 44: 507–18.
35. **Wojcikiewicz RJ.** Type I, II, and III inositol 1,4,5-trisphosphate receptors are unequally susceptible to down-regulation and are expressed in markedly different proportions in different cell types. *J Biol Chem.* 1995; 270: 11678–83.
36. **Roy A, Wonderlin WF.** The permeability of the endoplasmic reticulum is dynamically coupled to protein synthesis. *J Biol Chem.* 2003; 278: 4397–403.
37. **Flourakis M, Van Coppenolle F, Lehen'kyi V, *et al.*** Passive calcium leak via translocon is a first step for iPLA2-pathway regulated store operated channels activation. *FASEB J.* 2006; 20: 1215–7.
38. **Ong HL, Liu X, Sharma A, *et al.*** Intracellular Ca^{2+} release via the ER translocon activates store-operated calcium entry. *Pflugers Arch.* 2007; 453: 797–808.
39. **Walker ES, Martinez M, Brunkan AL, *et al.*** Presenilin 2 familial Alzheimer's disease mutations result in partial loss of function and dramatic changes in Abeta 42/40 ratios. *J Neurochem.* 2005; 92: 294–301.
40. **Stromberg K, Hansson EM, Laudon H, *et al.*** gamma-Secretase complexes containing N- and C-terminal fragments of different presenilin origin retain normal gamma-secretase activity. *J Neurochem.* 2005; 95: 880–90.
41. **Massey LK, Mah AL, Monteiro MJ.** Ubiquilin regulates presenilin endoproteolysis and modulates gamma-secretase components, Pen-2 and nicastrin. *Biochem J.* 2005; 391: 513–25.
42. **Campbell WA, Reed ML, Strahle J, *et al.*** Presenilin endoproteolysis mediated by an aspartyl protease activity pharmacologically distinct from gamma-secretase. *J Neurochem.* 2003; 85: 1563– 74.
43. **Cowburn RF, Popescu BO, Ankarcrona M, *et al.*** Presenilin-mediated signal transduction. *Physiol Behav.* 2007; 92: 93–7.
44. **Pack-Chung E, Meyers MB, Pettingell WP, *et al.*** Presenilin 2 interacts with sorcin, a modulator of the ryanodine receptor. *J Biol Chem.* 2000; 275: 14440–5.
45. **Lytton J, Westlin M, Burk SE, *et al.*** Functional comparisons between isoforms of the sarcoplasmic or endoplasmic reticulum family of calcium pumps. *J Biol Chem.* 1992; 267: 14483–9.
46. **Placanica L, Tarassishin L, Yang G, *et al.*** PEN2 and presenilin-1 modulate the dynamic equilibrium of presenilin-1 and presenilin-2 gamma -secretase complexes. *J Biol Chem.* 2008; 284: 2967–77.